J. Fluid Mech. (2010), *vol.* 659, *pp.* 484–504.
doi:10.1017/S0022112010002582

On higher order Bragg resonance of water waves by bottom corrugations

JIE YU[1]† AND LOUIS N. HOWARD[2]

[1]Department of Civil, Construction and Environmental Engineering, North Carolina State University, Raleigh, NC 27695-7908, USA

[2]Department of Mathematics, Massachusetts Institute of Technology, Cambridge, MA 02139, USA

(Received 14 July 2009; revised 28 April 2010; accepted 28 April 2010;
first published online 12 July 2010)

The exact theory of linearized water waves in a channel of indefinite length with bottom corrugations of finite amplitude (Howard & Yu, *J. Fluid Mech.*, vol. 593, 2007, pp. 209–234) is extended to study the higher order Bragg resonances of water waves occurring when the corrugation wavelength is close to an integer multiple of half a water wavelength. The resonance tongues (ranges of water-wave frequencies) are given for these higher order cases. Within a resonance tongue, the wave amplitude exhibits slow exponential modulation over the corrugations, and slow sinusoidal modulation occurs outside it. The spatial rate of wave amplitude modulation is analysed, showing its quantitative dependence on the corrugation height, water-wave frequency and water depth. The effects of these higher order Bragg resonances are illustrated using the normal modes of a rectangular tank.

Key words: coastal engineering, surface gravity waves, wave scattering

1. Introduction

The physical idea of Bragg resonance (sometimes also referred to as Bragg reflection or Bragg scattering) in the case of water waves can be illustrated by considering a linear water wave propagating over a series of well-submerged small sandbars (i.e. bottom corrugations) in otherwise constant water depth. Each bar crest can cause a little bit of reflection, individually negligible. However, when the bar spacing is close to half the water wavelength, reflections from successive crests are in phase and add up to form a strong reflected wave at the seaward side of the bar field. Continually losing energy to the scattered waves as it attempts to transit the bar field, the incident-wave amplitude decreases shorewards. While it originated in X-ray physics, the phenomenon in water waves has been well studied, e.g. Davies (1982), Davies & Heathershaw (1984), Mei (1985), Dalrymple & Kirby (1986), Kirby (1986), Liu (1987), Mei, Hara & Naciri (1988), Guazzelli, Rey & Belzons (1992), Rey, Guazzelli & Mei (1996), Liu & Yue (1998), Yu & Mei (2000*a*) and Alam, Liu & Yue (2009), to name only a few.

It seems that such accumulative, collaborative effects should also be expected when the bottom corrugations have a wavelength close to an integer multiple of half a water wavelength, as in those cases reflections from successive crests are also in phase. In X-ray studies, the Bragg condition is stated as $m\lambda_x = 2d\sin\theta$, where m is

† Email address for correspondence: jie_yu@ncsu.edu

an integer, λ_x is the X-ray wavelength, d is the spacing of the crystal planes and θ is the angle between the incident beam and the reflecting planes (Bragg & Bragg 1913). The equivalent (normal incident) wavelength $\lambda_x/\sin\theta$ gives the maximum reflection corresponding to $m = 1, 2, 3, \ldots$, referred to as the first, second, third, ... order reflections. In the water-wave analogue studied here, we consider only normally incident waves; so the Bragg condition reduces to $m\lambda = 2d$, with d being identified as the bottom-corrugation wavelength. For $m = 1$, this is the well-recognized Bragg resonance condition for water waves by half-wavelength sandbars in previous studies.

The picture depicted above, of reflections from successive bar crests reinforcing constructively, is effective to illustrate the general physical idea, but it can sometimes be misleading that Bragg resonance of water waves is all about incident waves being reflected, and the reflection coefficient over and upstream of a bar patch is the necessary measure of the effects of Bragg resonance. Reflections from successive bar crests occur equally to waves propagating in both directions (in the two-dimensional situation). Yu & Mei (2000*a*) have shown, using the asymptotic theory (Mei 1985), that linear standing waves in front of a vertical impermeable wall (e.g. seawall) can be altered significantly due to the Bragg resonance by a patch of small-amplitude sandbars, but reflection coefficients in these cases are everywhere unity due to the conservation of wave-energy fluxes in the absence of dissipation. The effects on the waves depend sensitively on the phase of the bottom wave at the location of the wall (Yu & Mei 2000*a*).

In our earlier study (Howard & Yu 2007; hereafter referred to as HY07), we developed an exact theory for linear irrotational motions over a corrugated bottom which have simple harmonic time dependence. The corrugations used there were a family characterized by arbitrary wavelength and amplitude parameters, and for small amplitude, the corrugations are nearly sinusoidal. The precise form is quoted in § 2. This choice was motivated mainly by mathematical convenience, but is no more special than any other two-parameter family. Such motions exist for any frequency and all of them can be obtained as linear combinations of a basic set of Floquet type of solutions, as was developed in HY07 and is described in § 2. However, in HY07 we examined in detail frequencies close to the $m = 1$ primary Bragg resonance only, and made comparisons with the asymptotic theory of Mei (1985), which assumes small amplitude of both water waves and corrugations, and a small deviation from the Bragg resonance frequency. We also made an application to examine the normal modes (i.e. standing waves) of a rectangular tank with a corrugated bottom which have natural frequencies close to the $m = 1$ Bragg resonance frequency, finding marked effects on the shape of the eigenfunctions (i.e. surface waveforms) consistent with the previous study (Yu & Mei 2000*a*).

The purpose of this paper is to explore the higher order Bragg resonances (occurring when the corrugation wavelength is close to an integer multiple of half a water wavelength, i.e. when $m > 1$) and demonstrate their effects using the normal modes of a tank with a corrugated bottom. The exact solutions in HY07 could be applied to many specific problems, other than the normal-mode problem, for instance to finding the reflection coefficient over a patch of corrugations in an otherwise flat bottom (a question which admittedly has been the focus or motivation of a number of earlier publications). However, neither here nor in HY07 do we discuss reflection coefficients.

It is worth emphasizing that nonlinearity of the wave itself is not necessary for Bragg resonance. Indeed, X-rays are regarded as short electromagnetic waves and so are described by the completely linear Maxwell equations. Water waves are always somewhat nonlinear, but many cases of real physical interest can be treated as

linear, or only weakly nonlinear. In HY07 and the present paper, we take strictly linear water waves, because we are then able to find exact solutions and remove the restriction of small-amplitude corrugations. The term 'higher order' in this paper refers back to the original X-ray work. In this sense, the terminology is rather more consistent with that used by Guazzelli *et al.* (1992) (but not really the same), who experimentally demonstrated the existence of the second-order ($m=2$) Bragg resonance. These experiments were carried out with carefully generated linear water waves over doubly sinusoidal bottoms.

There are certainly interesting phenomena resulting from water-wave nonlinearity tied in with Bragg resonance, e.g. Liu & Yue (1998) and Alam *et al.* (2009). In such studies, the term 'higher order Bragg resonance' was used, but it is in the sense of a perturbation expansion in terms of water wave and/or corrugation amplitude. Therefore, it has a different meaning from the terminology used in the present paper and in Guazzelli *et al.* (1992). It should also be mentioned that the classical wave–wave interaction theory (e.g. Phillips 1960, 1977) has been used to interpret Bragg resonance by treating the bottom corrugation as a wave with zero frequency, e.g. Mei (1985) and Liu & Yue (1998). This interpretation works for obtaining the Bragg condition for the first order ($m=1$) and is necessary when the focus is on the nonlinearity of the free surface as in Liu & Yue (1998). However, Bragg scattering is fundamentally a linear-wave phenomenon (i.e. superposition of waves), and does not necessarily follow the framework of nonlinear wave–wave interaction.

This paper is organized as follows. To be self-contained, in § 2 we shall first outline the formulation of the linear-water-wave problem in an infinite channel with periodic corrugations on the bottom, presenting some key results necessary for obtaining solutions for higher order Bragg resonances while referring details to HY07. In § 3, the solutions of the ranges of frequencies for exponential modulations (resonance tongues) for $m>1$ are discussed, and the similarity of these results to those of Mathieu's equation is remarked on. To illustrate the phenomena, the normal modes affected by higher order Bragg resonances in a rectangular tank are presented in § 4. Concluding remarks follow in § 5.

2. Linear water waves over bottom corrugations of finite amplitude

Let us consider the linear irrotational motions in an open channel. In the vertical plane (x, z), where x is along the channel and z points upwards with $z=0$ at the undisturbed water surface, the corrugated bottom is at $z=-h+h_b$, where h is the mean (constant) water depth and h_b is the profile of the bottom corrugations. From the linear-wave theory, the velocity potential $\phi(x, z, t)$ satisfies

$$\nabla^2\phi=0 \quad \text{for} \quad -h+h_b\leqslant z\leqslant 0, \quad -\infty<x<\infty, \tag{2.1}$$

$$\phi_z=\phi_x h_{b,x} \quad \text{at} \quad z=-h+h_b, \tag{2.2}$$

$$\phi_{tt}+g\phi_z=0 \quad \text{at} \quad z=0. \tag{2.3}$$

Following HY07, we shall take the corrugation profile to be

$$h_b=\epsilon h\cos 2\xi, \quad \text{where} \quad \xi-\epsilon k_B h\coth(2k_B h)\sin 2\xi=k_B x. \tag{2.4}$$

The corrugations are not exactly sinusoidal, but strictly periodic with a wavenumber $2k_B$, where k_B is the water wavenumber corresponding to the primary Bragg resonance frequency ω_B, i.e.

$$\omega_B^2=gk_B\tanh k_B h. \tag{2.5}$$

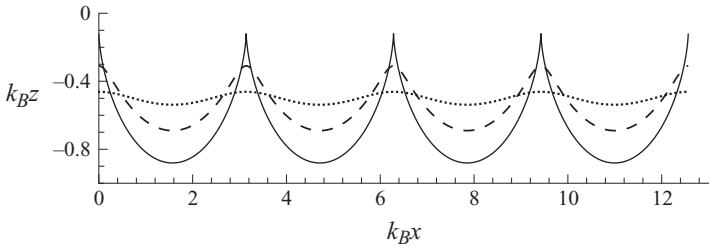

FIGURE 1. Profiles of bottom corrugations for different values of amplitude ϵ. $k_Bh = 0.5$; thus, $\epsilon_* = 0.7616$. $\cdots\cdots$, $\epsilon = 0.1\epsilon_*$; – – –, $\epsilon = 0.5\epsilon_*$; ——, $\epsilon = 1.0\epsilon_*$.

For small corrugation amplitude ϵ, $h_b \simeq \epsilon h \cos 2k_Bx$; as ϵ increases, the corrugations become increasingly cusp-like (see figure 1). The slope of the corrugation crests becomes infinite as $\epsilon \to \epsilon_*$, where

$$\epsilon_* = \tanh 2k_Bh/(2k_Bh). \tag{2.6}$$

We do not restrict ourselves to corrugations of infinitesimal amplitude; however, we do require $\epsilon < \epsilon_*$ so that the corrugation profile is single-valued. Since $\epsilon_* < 1$, the corrugation crests do not penetrate the free surface. As in HY07, we use a conformal map, i.e.

$$k_Bx = \xi - \epsilon b \sin 2\xi \cosh 2\eta, \qquad k_Bz = \eta - \epsilon b \cos 2\xi \sinh 2\eta, \tag{2.7a, b}$$

where

$$b = k_Bh/\sinh(2k_Bh). \tag{2.8}$$

This maps the undisturbed free surface $z = 0$ onto $\eta = 0$ and the bottom $z = -h + h_b$ onto $\eta = -k_Bh$, making the actual flow domain a strip on the mapped plane.

2.1. *Floquet solutions*

For a periodic motion with simple harmonic time dependence, we set $\phi = \varphi(\xi, \eta)\mathrm{e}^{-\mathrm{i}\omega t} +$ c.c., where ω is the angular frequency. The solution of φ can be constructed as superpositions of Floquet solutions, which have the form of a periodic function of ξ multiplied by an exponential in ξ, i.e.

$$\varphi = \mathrm{e}^{\mu\xi} \sum_{n=-\infty}^{\infty} D_n \mathrm{e}^{\mathrm{i}n\xi} \frac{\cosh\left[(n - \mathrm{i}\mu)(\eta + k_Bh)\right]}{\cosh\left[(n - \mathrm{i}\mu)k_Bh\right]}. \tag{2.9}$$

The Fourier coefficients D_n satisfy the recurrence relationship

$$L_nD_n = D_{n-2} + D_{n+2}, \tag{2.10}$$

$$L_n := -(\epsilon b\lambda)^{-1}\left\{(n - \mathrm{i}\mu)\tanh\left[(n - \mathrm{i}\mu)k_Bh\right] - \lambda\right\}, \tag{2.11}$$

where

$$\lambda = \omega^2/gk_B \tag{2.12}$$

is a dimensionless measure of angular frequency. The three-term recursion (2.10) comes from the free-surface boundary condition (2.3) after transforming to the (ξ, η) plane. The Floquet exponent μ is complex in general. The representation of (2.9) using even n is not coupled with that using odd n, and without any loss of generality we can require $-1 < \mathrm{Im}\,\mu \leqslant 1$ (cf. HY07). Equations (2.9)–(2.11) can be solved using continued fractions.

For any given frequency ω, there are two Floquet solutions whose linear combinations are analogous to the linear combinations of the left-going and right-going propagating waves on a flat bottom. (The Floquet solutions are not individually analogous to either of the propagating waves; cf. HY07.) Corresponding to the frequency ω, there are also two families of Floquet solutions, each of which has infinite numbers. The Floquet exponents are real and rather close to the appropriate exponents of the two families of evanescent modes for the flat-bottom channel (i.e. the roots $\pm\kappa_n$ of the equation $\omega^2 = -g\kappa_n \tan \kappa_n h$). These evanescent modes do not have direct analogues in the asymptotic theory (Mei 1985), because they are not slowly varying in x, even for small-amplitude corrugations. They did, however, appear in the pioneering paper of Davies & Heathershaw (1984), which dealt with scattering of a plane water wave by a finite patch of corrugations. They solved it quite completely within the scope of regular perturbation theory, by a Fourier transform method. Davies & Heathershaw referred to these evanescent waves as 'trapped waves', located at and near the ends of the corrugation patch.

The Floquet exponents are determined by a continued fraction relation, analogous to the dispersion relation for water waves over a flat bottom. For mathematical details we refer to HY07 and we quote here only the key solutions from which extension to higher order Bragg resonances can be made readily.

2.2. *Floquet exponents*

For the modes using the representation with odd n in (2.9), the possible Floquet exponents μ must satisfy

$$CF_1(\mu)CF_1(-\mu) = 1, \tag{2.13}$$

where the continued fraction $CF_1(\mu)$ follows the definition

$$CF_j(\mu) = \cfrac{1}{L_j(\mu) - \cfrac{1}{L_{j+2}(\mu) - \cfrac{1}{L_{j+4}(\mu) - \cdots}}}, \quad j = 1, 2, 3, \ldots . \tag{2.14}$$

For the modes using the representation with even n in (2.9), the possible Floquet exponents μ must satisfy

$$L_0(\mu) = CF_2(\mu) + CF_2(-\mu). \tag{2.15}$$

We note that $L_j(-\mu) = L_{-j}(\mu)$ and $CF_j(-\mu) = CF_{-j}(\mu)$.

Either representation, with even or odd n in (2.9), can be used to construct the solution of a mode (propagating or evanescent wave). However, one representation may be more convenient than the other, depending on the modes considered. For example, in examining the primary Bragg resonance, HY07 found that it is convenient to use the odd representations for the propagating modes whose frequencies are close to the Bragg resonance ω_B. From (2.13), the Floquet exponents are determined, which are real for the exponentially modulated waves and pure imaginary for sinusoidally modulated waves. The corresponding evanescent modes, when represented using even n, have a sequence of real Floquet exponents $\mu_1, \mu_2, \ldots$ (and their negatives $-\mu_1, -\mu_2, \ldots$), which can be readily computed from (2.15). The continued fractions are calculated following the usual algorithm outlined in HY07.

3. Resonance tongues for propagating modes

For corrugations of wavenumber $2k_B$, we define the Bragg resonance water wavenumbers as

$$k_{Bm} = mk_B, \quad m = 1, 2, 3, \ldots, \tag{3.1}$$

and the corresponding Bragg resonance frequencies as

$$\omega_{Bm}^2 = gk_B\lambda_{Bm}, \qquad \lambda_{Bm} = m \tanh mk_B h, \quad m = 1, 2, 3, \ldots. \tag{3.2}$$

Bragg resonance occurs when the water wavenumber $k \simeq k_{Bm}$, i.e. when $m/2$ water wavelength is close to the corrugation wavelength. Specifically, in certain ranges of frequencies, which depend on the corrugation amplitude and are near a Bragg resonance frequency, the Floquet exponents for the propagating modes are real (i.e. a positive μ and its opposite). These are waves of exponential modulation over the corrugations. These ranges of frequencies for exponential modulation are called resonance tongues. Outside a resonance tongue (still sufficiently close to the Bragg resonance frequency ω_{Bm}), the Floquet exponents are opposite imaginary numbers, and the wave amplitudes exhibit slow oscillatory modulation as the waves transit the corrugations. For primary Bragg resonance ($m = 1$), $k_{B1} = k_B$ and $\omega_{B1} = \omega_B$. The second subscript will therefore be suppressed when referring to the primary Bragg resonance frequency and the wavenumber. Obviously, ω_{Bm} increases with m, and higher order Bragg resonances are important to higher frequency modes (with shorter wavelengths).

For propagating modes of frequency close to the mth Bragg resonance, it is expected that the Floquet solutions will resemble the flat-bottom propagating modes with wavenumbers near k_{Bm}, and so the dominant Fourier coefficients in (2.9) should be D_m and D_{-m}. Thus, when m is odd, e.g. the primary and tertiary Bragg resonances, the representation with odd n is more convenient. When m is even, on the other hand, the representation with even n is preferred. Consequently, we determine the Floquet exponents μ for the propagating modes using (2.13) when m is odd and using (2.15) when m is even. In all cases, for evanescent waves the representation with even n is always preferred, the D_0 term in the Fourier series always being important. The Floquet exponents for evanescent waves are not small even for small ϵ.

For ω sufficiently close to ω_B, HY07 found that (2.13) indeed has pure real solutions of μ for $0 < \epsilon \leqslant \epsilon_*$. As ω moves away from ω_B, becoming either smaller or greater, the Floquet exponent μ approaches zero and then becomes pure imaginary, corresponding to the waves of sinusoidal modulation outside the resonance tongue. The lower and upper frequencies corresponding to $\mu = 0$, i.e. ω_{c-} and ω_{c+}, define the boundaries of the resonance tongue. These features of Floquet exponents will be similarly retained for $m > 1$ when the wave frequency ω is close to ω_{Bm}. However, for $m > 1$ directly solving (2.13) or (2.15) presents numerical difficulty. For the mth Bragg resonance, as $\epsilon \to 0$, $\lambda \to \lambda_{Bm}$. Recall that $\omega/\omega_{Bm} = (\lambda/\lambda_{Bm})^{1/2}$. From (2.11), $L_m \to 0$ as $\omega \to \omega_{Bm}$. L_m is one of the partial denominators of the continued fraction CF_m, which makes CF_m singular for the solutions of μ sought as $\epsilon \to 0$. Appropriate re-arrangements of (2.13) and (2.15) are needed to avoid direct calculation of the 'troubling' continued fractions as follows.

For secondary Bragg resonance ($m = 2$), we rewrite (2.15) by expanding CF_2 in terms of CF_4, i.e.

$$L_0(\mu)\,[L_2(\mu) - CF_4(\mu)]\,[L_2(-\mu) - CF_4(-\mu)] = L_2(-\mu) - CF_4(-\mu) + L_2(\mu) - CF_4(\mu). \tag{3.3}$$

This form is well behaved numerically close to ω_{B2}, and is used to determine μ for the propagating modes for $m=2$. Equation (2.15) is also the basic condition for determining μ for quaternary Bragg resonance ($m=4$). As $\omega \to \omega_{B4}$, CF_4 becomes singular. One shall then rewrite (3.3) further, expanding CF_4 in terms of L_4 and CF_6 to obtain the appropriate form for $m=4$. The mathematics is tedious, but straightforward. The details are omitted here for brevity. For tertiary Bragg resonance ($m=3$), we shall rewrite (2.13), to avoid direct calculation of $CF_3(\mu)$, as follows:

$$[L_1(\mu)L_1(-\mu)-1]\,[L_3(\mu)-CF_5(\mu)]\,[L_3(-\mu)-CF_5(-\mu)]$$
$$= L_1(-\mu)\,[L_3(-\mu)-CF_5(-\mu)] + L_1(\mu)\,[L_3(\mu)-CF_5(\mu)] - 1. \quad (3.4)$$

This is used to solve for μ for the propagating modes close to ω_{B3}. The process just outlined can, in theory, be continued to deal with even higher values of m. However, as will be seen in § 3.2, the effects of Bragg resonance become increasingly weaker as m gets higher since the waves become increasingly shorter. The practical interest of these much higher order resonances may be limited. In (3.3) and (3.4), the continued fractions are evaluated using the usual algorithm.

We shall present and discuss in § 3.2 the numerical results of resonance tongues, making comparisons. For small ϵ, approximate solutions can be obtained analytically by applying the perturbation analysis to (2.13) and (2.15). These perturbation solutions explicitly demonstrate the dependence of resonance tongues on corrugation amplitude ϵ as m increases. They also provide a check on the numerical results. We thus present these perturbation solutions in the next section, and then proceed to the numerical results.

3.1. *Small ϵ behaviour*

First consider the case $m=2$. Also $\lambda_{B2}=2\tanh 2k_Bh$. As $\omega \to \omega_{B2}$, $\lambda \to \lambda_{B2}$. From (2.11), $L_0(\mu) \sim (\epsilon b)^{-1}$, where b is defined in (2.8). For (2.15) to have a solution as $\epsilon \to 0$ and $\mu \to 0$, $CF_2(\mu)$ must have the same ϵ^{-1} singularity. Since $CF_2 = [L_2 - CF_4]^{-1}$ and $CF_4(\mu) = O(\epsilon b)$, we must then conclude that $L_2(\mu) = O(\epsilon b)$. This can be met if μ approaches zero and λ approaches λ_{B2} in the manner

$$\mu = 0 + (\epsilon b)^2 A + \cdots, \qquad \lambda/\lambda_{B2} = 1 + (\epsilon b)^2 C + \cdots. \quad (3.5)$$

Substituting this into (3.3), the leading order perturbation expansion is $O(\epsilon)$ and leads to

$$A^2\left[\tfrac{1}{2} + 2k_Bh/\sinh 4k_Bh\right]^2 + \left[C - (1-\lambda_{B4}/\lambda_{B2})^{-1} - 1\right]^2 = 1. \quad (3.6)$$

Since $\omega/\omega_{B2} = (\lambda/\lambda_{B2})^{1/2}$, when $\mu=0$, $A=0$, and we obtain the lower and upper frequencies at the boundaries of the resonance tongue, i.e.

$$\omega_{c\mp}/\omega_{B2} = \sqrt{1 + (\epsilon b)^2 C_\mp + \cdots},$$

where

$$C_- = (1-\lambda_{B4}/\lambda_{B2})^{-1}, \qquad C_+ = 2 + (1-\lambda_{B4}/\lambda_{B2})^{-1}. \quad (3.7)$$

The separation of ω_{c-} and ω_{c+} gives the width of the resonance tongue, i.e. for $m=2$,

$$(\omega_{c+} - \omega_{c-})/\omega_{B2} = (\epsilon b)^2. \quad (3.8)$$

For the case $m=3$, $\lambda_{B3}=3\tanh 3k_Bh$. As $\lambda \to \lambda_{B3}$, $L_1(\mu) \sim (\epsilon b)^{-1}$. $CF_1(\mu)$ and $CF_1(-\mu)$ must be of $O(1)$ as $\mu \to 0$ in order for (2.13) to have a solution. Since $CF_1(\mu) = [L_1(\mu) - CF_3(\mu)]^{-1}$, it is clear that $CF_3(\mu)$ must have the same $(\epsilon b)^{-1}$

singularity to balance $L_1(\mu)$. Consequently, $L_3(\mu) \sim \epsilon b$. This indicates that for small ϵ,

$$\mu = 0 + (\epsilon b)^3 A + \cdots, \qquad \lambda/\lambda_{B3} = 1 + (\epsilon b)^2 B + (\epsilon b)^3 C + \cdots. \tag{3.9}$$

Substituting this into (3.4), we obtain the following at the leading order $O(1/\epsilon b)$:

$$B = (1 - \lambda_{B1}/\lambda_{B3})^{-1} + (1 - \lambda_{B5}/\lambda_{B3})^{-1}, \tag{3.10}$$

and at $O(1)$,

$$A^2 \left(\tfrac{1}{3} + 2k_B h / \sinh 6k_B h\right)^2 + C^2 = (1 - \lambda_{B1}/\lambda_{B3})^{-4}. \tag{3.11}$$

When $\mu = 0$, $A = 0$, and the lower and upper frequencies at the boundaries of the resonance tongue are

$$\omega_{c\mp}/\omega_{B3} = \sqrt{1 + (\epsilon b)^2 B \mp (\epsilon b)^3 (1 - \lambda_{B1}/\lambda_{B3})^{-2} + \cdots}. \tag{3.12}$$

The width of the resonance tongue for $m = 3$ is

$$(\omega_{c+} - \omega_{c-})/\omega_{B3} = (\epsilon b)^3 (1 - \lambda_{B1}/\lambda_{B3})^{-2}. \tag{3.13}$$

Similarly, we can obtain the perturbation solution for the case $m = 4$. The algebra becomes increasingly tedious since higher order expansions in ϵb must be carried out to obtain the significant results. We shall omit the details and quote the results as follows:

$$\mu = 0 + (\epsilon b)^4 A + \cdots, \qquad \lambda/\lambda_{B4} = 1 + (\epsilon b)^2 B + (\epsilon b)^4 C + \cdots, \tag{3.14}$$

where

$$B = (1 - \lambda_{B2}/\lambda_{B4})^{-1} + (1 - \lambda_{B6}/\lambda_{B4})^{-1}, \tag{3.15}$$

$$A^2 \left(\tfrac{1}{4} + 2k_B h / \sinh 8k_B h\right)^2 + (C - \mathscr{P})^2 = (1 - \lambda_{B2}/\lambda_{B4})^{-4}, \tag{3.16}$$

$$\begin{aligned} \mathscr{P} \;=\; & -B^3 + 2B^2 + 2B (1 - \lambda_{B2}/\lambda_{B4})^{-1} (1 - \lambda_{B6}/\lambda_{B4})^{-1} \\ & + (1 - \lambda_{B6}/\lambda_{B4})^{-2} (1 - \lambda_{B8}/\lambda_{B4})^{-1} + (1 - \lambda_{B2}/\lambda_{B4})^{-2}. \end{aligned}$$

The width of the resonance tongue for $m = 4$ is

$$(\omega_{c+} - \omega_{c-})/\omega_{B4} = (\epsilon b)^4 (1 - \lambda_{B2}/\lambda_{B4})^{-2}. \tag{3.17}$$

A few observations can be made immediately. First, the Floquet exponent μ, which gives the spatial growth (or decay) rate of amplitude modulation, and the width of the resonance tongue are both of $O(\epsilon^m)$. For a fixed corrugation amplitude ϵ, the range of frequencies for exponential modulation becomes increasingly narrower for higher order Bragg resonances, and the wave amplitude becomes less variable in space. This is because the waves for the mth Bragg resonance become shorter as m increases, and hence are less affected by the bottom topography. Second, the centre of the resonance tongue is skewed increasingly towards the higher frequency side of ω_{Bm} as ϵ increases. In fact, when $m = 3$ and $m = 4$, $B < 0$ for sufficiently small $k_{Bm}h$, and thus, the Bragg resonance frequency ω_{Bm}, as is defined in (3.2), is outside the resonance tongue, corresponding to a sinusoidal modulation. Third, $\mathrm{d}/\mathrm{d}\epsilon\,(\omega_{c+})$ and $\mathrm{d}/\mathrm{d}\epsilon\,(\omega_{c-})$ are both of $O(\epsilon)$ in all cases for $m > 1$. Thus, for $m > 1$, the slopes of the boundaries of the resonance tongue approach zero as $\epsilon \to 0$ and are equal to zero at $\epsilon = 0$, suggesting that the resonance tongue is cusp-like, in the parameter plane ϵ–ω, not wedge-like as it is in the case $m = 1$. The cusp becomes sharper as m increases. As a last remark, the fact that both μ and the width of the resonance tongue are

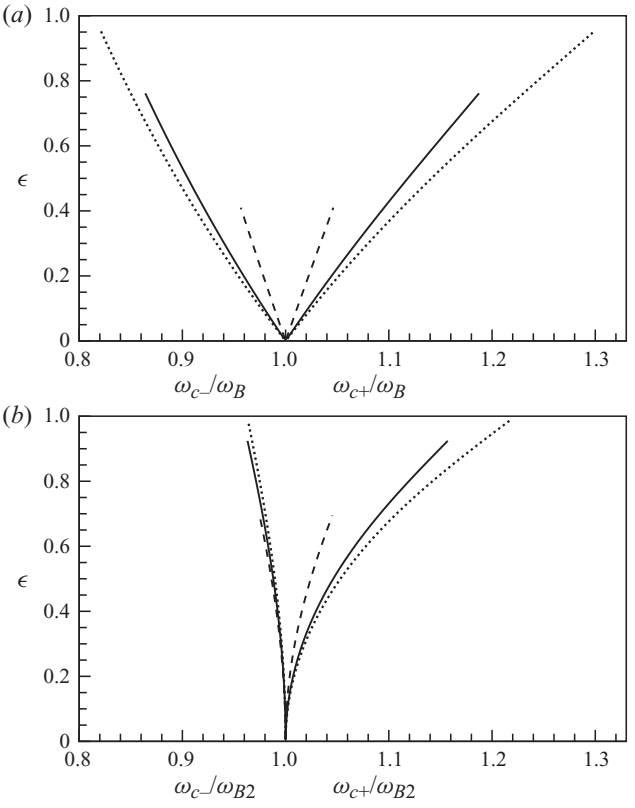

FIGURE 2(a, b). For caption see next page.

of $O(\epsilon^m)$ indicates that if an asymptotic theory for small-amplitude corrugation is to be adapted for higher order Bragg resonances, the analysis has to be carried out to $O(\epsilon^m)$ to obtain any significant results. As a check, we have indeed extended the theory in Mei (1985) to the cases $m > 1$, working, however, in the (ξ, η) plane, and reproduced the results presented in § 3.1 at the appropriate orders.

3.2. *Results*

As discussed above, using the appropriate form equivalent to either (2.13) when m is odd or (2.15) when m is even, one can obtain the Floquet exponents μ for the propagating modes of both exponential and sinusoidal modulations. In figure 2, ω_{c-}/ω_{Bm} and ω_{c+}/ω_{Bm} are plotted against ϵ for $k_{Bm}h = 0.2$, 0.5 and 1.2. Recall that $\epsilon = a/h$, where a is the dimensional corrugation amplitude. $\epsilon < \epsilon_*$ and ϵ_* varies with $k_B h$. For completeness and for comparison, the primary Bragg resonance ($m = 1$) is included.

Comparing with $m = 1$, resonance tongues for $m > 1$ are, in general, much narrower. The resonance tongues are indeed cusps at all water depths for $m > 1$, while they are approximately wedges for $m = 1$. For small ϵ, the width of the cusps is proportional to ϵ^m, as indicated by the perturbation solutions in § 3.1. In all cases, including $m = 1$, for small and moderate water depths the resonance tongues are asymmetric with respect to the Bragg resonance frequency ω_{Bm}, extending considerably more into the higher frequency side of ω_{Bm}. For $m = 3$ and $m = 4$, ω_{Bm} is outside the resonance tongue unless $k_{Bm}h$ or ϵ is sufficiently large. Given a water depth, say $k_{Bm}h = 0.5$, the

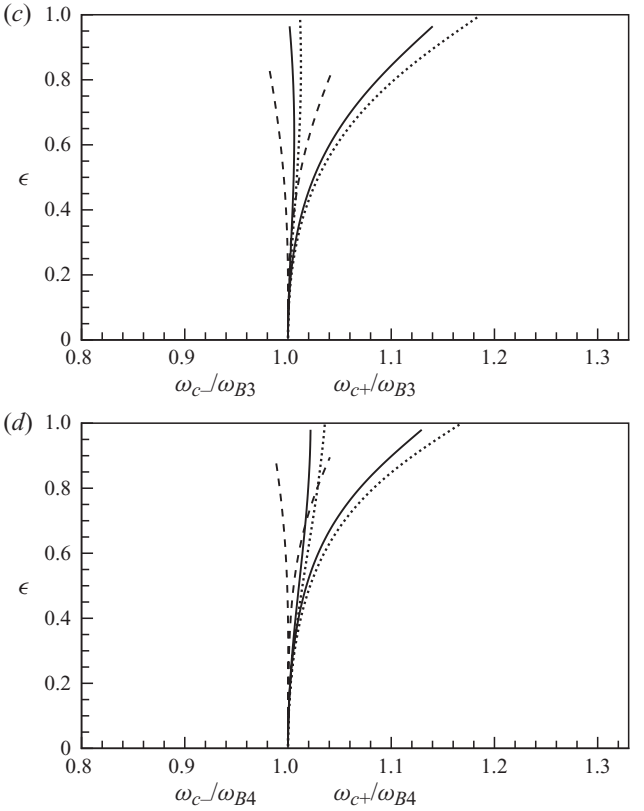

FIGURE 2. Graphs of ω_{c-}/ω_{Bm} and ω_{c+}/ω_{Bm} as functions of ϵ for water depth: $\cdots\cdots$, $k_{Bm}h = 0.2$; ——, $k_{Bm}h = 0.5$; – – –, $k_{Bm}h = 1.2$. (*a*) Primary Bragg resonance ($m = 1$); (*b*) secondary Bragg resonance ($m = 2$); (*c*) tertiary Bragg resonance ($m = 3$); (*d*) quaternary Bragg resonance ($m = 4$).

resonance tongue narrows as m increases, for all values of ϵ, indicating weaker effects of higher order Bragg resonances. Consider the corrugations of wavenumber $2k_B$. The waves affected by the mth Bragg resonance become increasingly shorter than the corrugation wavelength as m gets greater, even though the relative water depth $k_{Bm}h$ is kept the same. The bottom appears to be increasingly smooth, and further away, to the waves of interest as m increases, and hence less interaction occurs between the two. For the same reason, we observe the resonance tongue narrowing when the water depth increases for a given m.

For propagating modes close to ω_{Bm}, the Floquet exponents μ are real inside the resonance tongue and pure imaginary outside it. Thus, μ^2 is convenient for display both inside ($\mu^2 > 0$) and outside ($\mu^2 < 0$), as is done in HY07. In figures 3–6, we show the graphs of μ^2 as a function of ω/ω_{Bm} for various values of $k_{Bm}h$ and ϵ. For each case m, the water depths are $k_{Bm}h = 0.2$, 0.5 and 0.9. As indicated in the captions, somewhat larger values of ϵ are used for higher m due to the weaker effects of Bragg resonances. The graphs are generally similar, except for the magnitudes. For $m = 1$, the maximum real μ occurs at a frequency fairly close to ω_B for different values of ϵ. For $m > 1$, this maximum shifts towards higher frequencies as we increase ϵ, consistent with the asymmetry of the resonance tongues observed in figure 2.

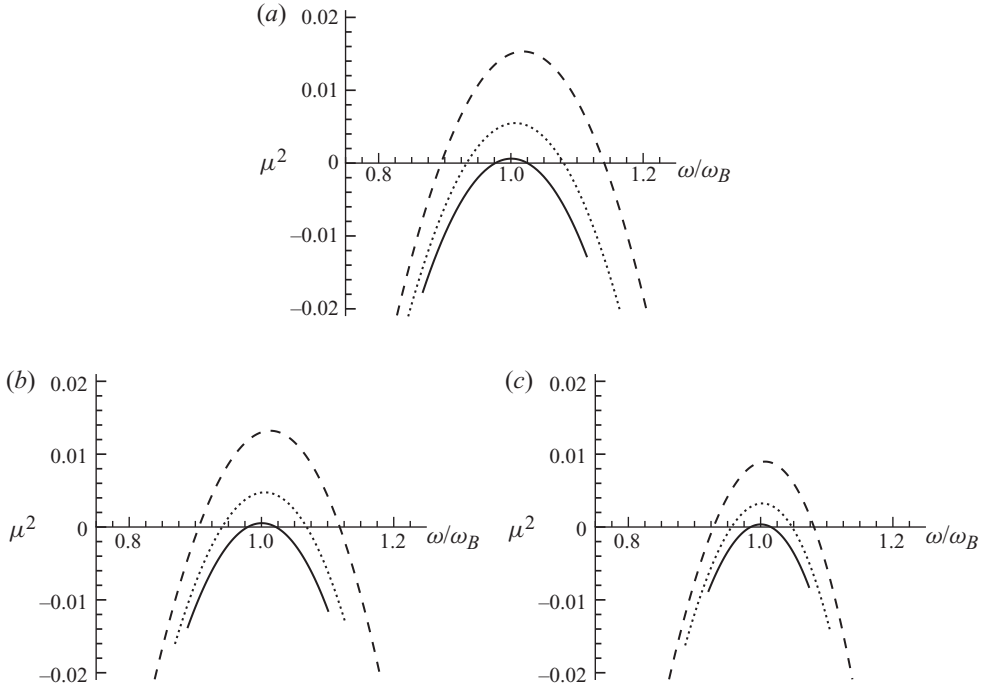

FIGURE 3. Graphs of μ^2 as a function of ω/ω_B for primary Bragg resonance ($m=1$). (a) $k_Bh=0.2$; (b) $k_Bh=0.5$; (c) $k_Bh=0.9$. For each k_Bh: ——, $\epsilon=0.1$; · · · · · ·, $\epsilon=0.3$; – – –, $\epsilon=0.5$.

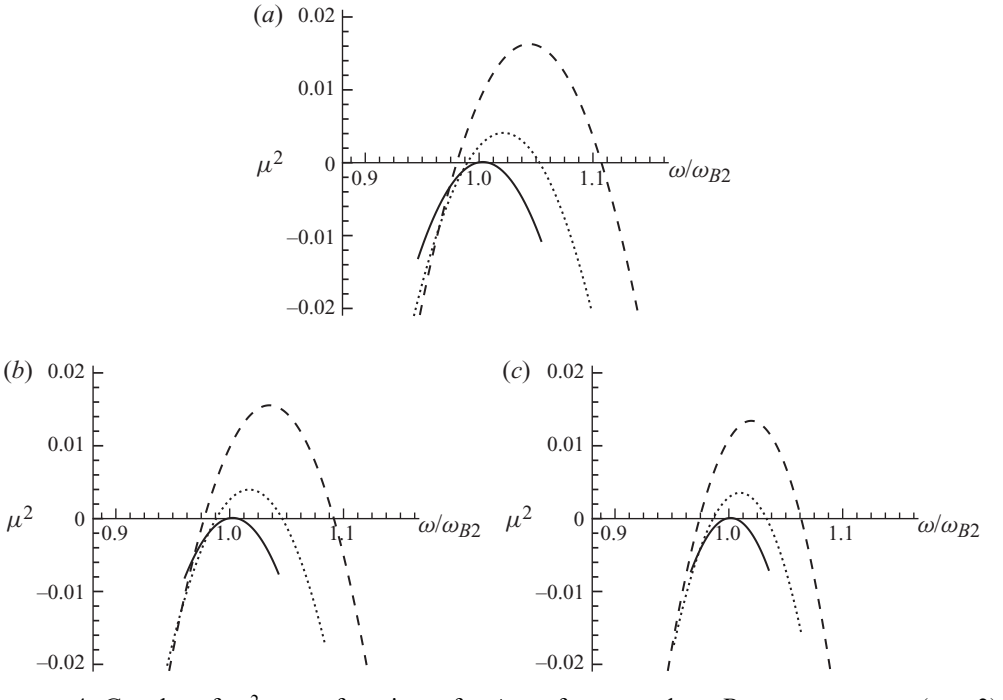

FIGURE 4. Graphs of μ^2 as a function of ω/ω_{B2} for secondary Bragg resonance ($m=2$). (a) $k_{B2}h=0.2$; (b) $k_{B2}h=0.5$; (c) $k_{B2}h=0.9$. For each $k_{B2}h$: ——, $\epsilon=0.2$; · · · · · ·, $\epsilon=0.5$; – – –, $\epsilon=0.7$.

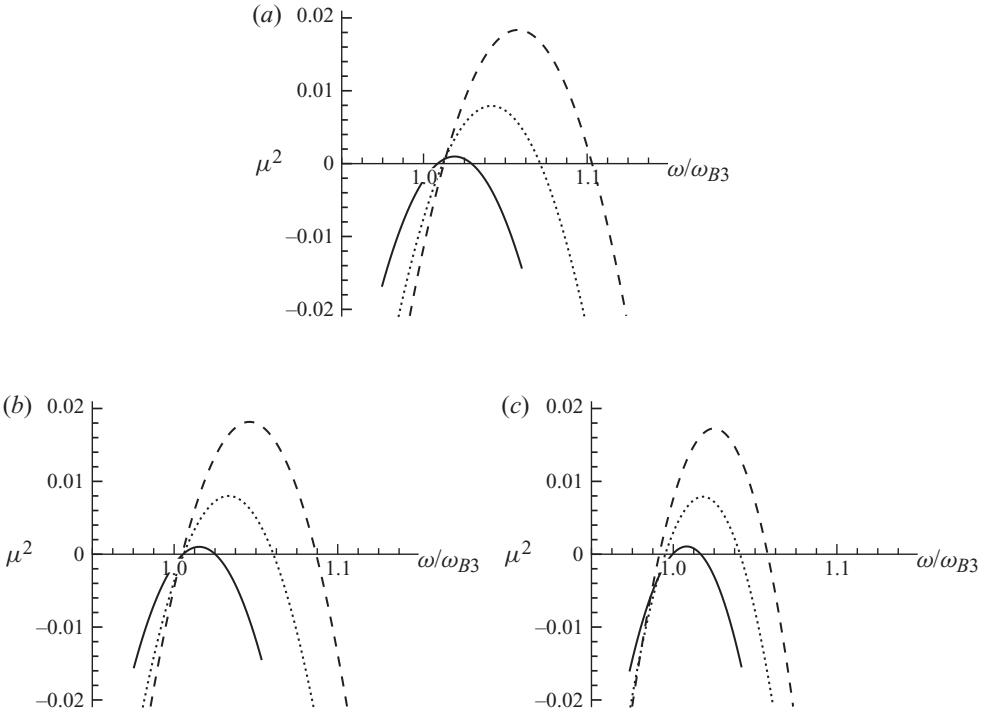

FIGURE 5. Graphs of μ^2 as a function of ω/ω_{B3} for tertiary Bragg resonance ($m=3$). (*a*) $k_{B3}h=0.2$; (*b*) $k_{B3}h=0.5$; (*c*) $k_{B3}h=0.9$. For each $k_{B3}h$: ——, $\epsilon=0.5$; ·····, $\epsilon=0.7$; – – –, $\epsilon=0.8$.

For exponential modulation, μ gives the amplitude growth (or decay) rate in ξ in the mapped plane, as well as in $k_B x$ in the x–z plane (cf. HY07). To fix the idea, take, for example, $\mu=0.1$, which is typical in figures 3–6. This gives an e-folding distance $10/\pi$ corrugation wavelengths, that is the wave amplitude can be amplified (or reduced) by a factor of e in a distance of approximately three corrugation wavelengths. In terms of the wave energy density, the factor is $e^2 \simeq 7$.

The set of Floquet solutions, whose existence and construction we have just described, forms a basis for all solutions of Laplace's equation satisfying the surface and bottom boundary conditions and periodic in time with a given frequency. They can be used to attack different problems involving linear water waves over a finite number of corrugations, when appropriate end boundary conditions are prescribed. It should, however, be stressed that the rate of exponential modulation (Floquet exponent) is determined by the corrugation amplitude, the water-wave frequency and by the water depth, being independent of the end conditions of a finite corrugation patch. In § 4, we shall demonstrate the effects of those higher order Bragg resonances that use the normal modes of a finite channel with vertical ends, as an example.

3.3. *Remarks on the similarity to Mathieu's equation*

The standard form of Mathieu's equation (Abramowitz & Stegun 1964) is

$$y'' + (a - 2q\cos 2x)\, y = 0. \tag{3.18}$$

Mathieu encountered it while studying the normal modes of an elliptical membrane, after separation of variables in the Helmholtz equation transformed to elliptical

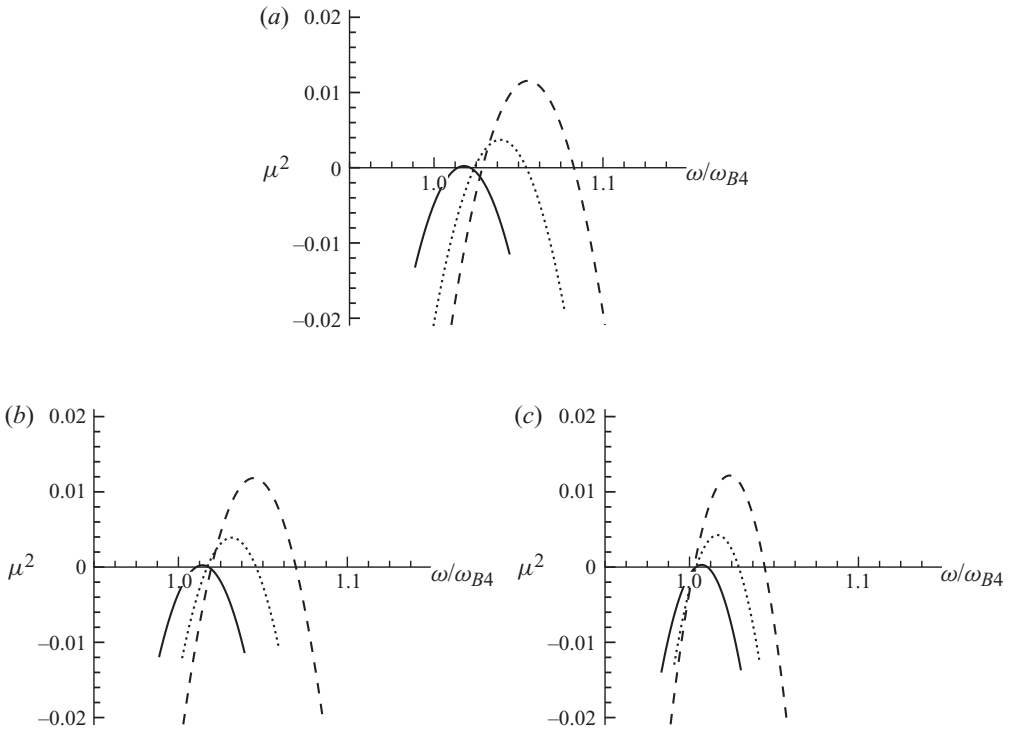

FIGURE 6. Graphs of μ^2 as a function of ω/ω_{B4} for quaternary Bragg resonance ($m=4$). (*a*) $k_{B4}h=0.2$; (*b*) $k_{B4}h=0.5$; (*c*) $k_{B4}h=0.9$. For each $k_{B4}h$: ——, $\epsilon=0.5$; · · · · · ·, $\epsilon=0.7$; – – –, $\epsilon=0.8$.

coordinates (Mathieu 1868). The relevant solutions in such a case are those periodic in x and may be regarded as eigenfunctions of (3.18) with periodic boundary conditions. For $q>0$, there are two distinct eigenvalues, $a=a_r(q)$ and $a=b_r(q)$, which merge into the degenerate eigenvalues $a_r=r^2$ (with eigenfunctions $\cos rx$ and $\sin rx$) as $q\to 0$. Graphs of these can be seen in figure 20.1 in Abramowitz & Stegun (1964). They bear a striking resemblance to the resonance tongue boundaries $\omega_{c\pm}$ in figure 2 in this paper, which also correspond to periodic solutions. The separation between a_r and b_r, for small q, is of $O(q^r)$, just as the width of our resonance tongues is of $O(\epsilon^m)$. In fact, Mathieu's equation has Floquet solutions with real exponents between a_r and b_r and imaginary exponents outside.

These similarities are not an accident. If we look for Floquet solutions of (3.18) in the form $y=e^{\mu x}\sum_{-\infty}^{\infty} D_n \mathrm{e}^{\mathrm{i}nx}$, we find the recurrence $\hat{L}_n D_n = D_{n+2}+D_{n-2}$, where $\hat{L}_n = q^{-1}[a-(n-\mathrm{i}\mu)^2]$, just like our recurrence (2.10) with L_n defined in (2.11). For small k_Bh, $L_n=\hat{L}_n$ if we identify q with $\epsilon b\lambda/k_Bh$ and a with λ/k_Bh. Of course, this small k_Bh approximation always fails for large enough n, however small k_Bh might be, nor do we necessarily want to have small k_Bh; so the problems are not identical, but there seems to be a real basis for some similarity. The normal modes we are studying here cannot be found by the simple separation of variables technique that applies to those of the elliptical membrane, and we do not have an analogue of the ordinary differential equation (3.18). However, because the general ideas of Floquet theory apply to both problems, we do find similar recurrences and similar continued fractions. We have confirmed that for $k_Bh\to 0$ the solutions in § 3.1 for small ϵ indeed

agree with the results given in chapter 20 in Abramowitz & Stegun (1964) when q and a are so identified, as mentioned above.

That there is some relationship between water-wave Bragg resonance and Mathieu's equation has been noted previously (Davies, Guazzelli & Belzons 1989; Kirby 1989). With various approximations, but always including small corrugation amplitude, Mathieu's equation has been obtained directly from the water-wave Bragg-resonance problem. As just remarked, it does not seem possible to do this with a finite corrugation amplitude, but the overall similarity still holds, e.g. the tilting towards higher frequencies of resonance tongues seen in figure 2 for all m is also found in the Mathieu equation.

4. Normal modes of a tank with corrugated bottom

A general solution for linearized motion of angular frequency ω is

$$\varphi = C^-\varphi^- + C^+\varphi^+ + \sum_{j=1,K} (C_j^-\varphi_j^- + C_j^+\varphi_j^+), \tag{4.1}$$

where $\varphi^{\pm}$ are the Floquet solutions for the two propagating modes, corresponding to μ and $-\mu$ (either real or pure imaginary), and $\varphi_j^{\pm}$ are the evanescent modes corresponding to the sequence of Floquet exponents μ_j and $-\mu_j$, $j = 1, 2, \ldots$, for the same frequency ω. For a normal mode, the coefficients C are to be determined so that the normal component of velocity vanishes everywhere on each endwall of the tank. In general, this will require an infinite number of the evanescent waves; in practice, we have to truncate the series at some finite number K, depending on how much inaccuracy in satisfying the endwall conditions is regarded as acceptable. A vertical endwall ($x =$ constant) in the (x, z) variables is usually not vertical in (ξ, η); it is only where the endwall is located exactly at a corrugation crest or trough that its image on the mapped plane appears vertical. Because the mapping (2.7) is conformal, the endwall condition remains that the normal derivative of φ is zero, but it must be applied on the actual image of the wall. Thus, the evanescent waves always seem to be needed to satisfy the endwall conditions, except for $\epsilon = 0$. The method for constructing the normal modes for $m = 1$ is detailed in HY07, and is applicable for $m > 1$. We emphasize here those higher frequency normal modes on which the higher order Bragg resonances have significant effects.

We have examined a number of examples for $m = 2$, 3 and 4, focusing on exponential modulations. Some are discussed here. Let the total length of the tank be L, and the two vertical endwalls be at $x = x_0$ and $x = L + x_0$. We define

$$\alpha = k_B x_0, \qquad -\pi/2 < \alpha \leqslant \pi/2, \tag{4.2}$$

$$\beta = k_B L - N\pi + \alpha, \qquad -\pi/2 \leqslant \beta - \alpha < \pi/2, \tag{4.3}$$

where N is the integer number of corrugation wavelengths nearest to the actual length of the tank. The parameters α and β, respectively, measure the phases of the left and right endwalls relative to the corrugation crest. For example, if the left endwall is at a corrugation trough, $\alpha = \pi/2$. The choice of N is so made that the normal mode to be constructed will tend to the Nth mode of the flat bottom case as $\epsilon \to 0$ for the case $m = 1$ (cf. HY07).

We first show examples with 16 corrugations, i.e. $N = 16$. In figure 7, the profiles of the surface elevation (at $t = 0$) are shown for secondary Bragg resonance ($m = 2$). Also $k_{B2}h = 0.5$ and $\epsilon = 0.3$ (i.e. $\epsilon/\epsilon_* = 0.3246$). For tertiary Bragg resonance ($m = 3$), the

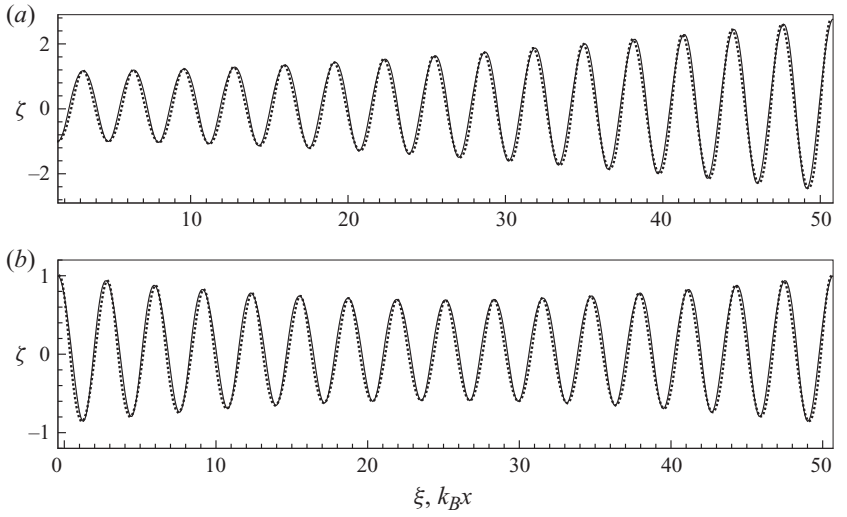

FIGURE 7. The profiles of the surface elevation (at $t=0$) for secondary Bragg resonance ($m=2$): ——, as a function of ξ; ·····, as a function of $k_B x$. Parameters are $k_{B2}h=0.5$, $\epsilon=0.3$, $N=16$. (*a*) $\alpha=\pi/2$, $\beta=17\pi/127$; (*b*) $\alpha=-\pi/10$, $\beta=-\alpha$.

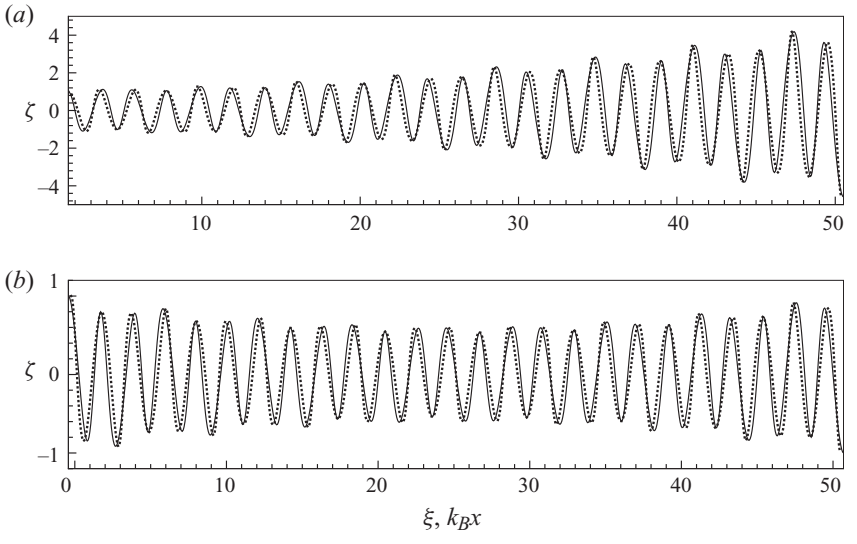

FIGURE 8. The profiles of the surface elevation (at $t=0$) for tertiary Bragg resonance ($m=3$): ——, as a function of ξ; ·····, as a function of $k_B x$. Parameters are $k_{B3}h=0.5$, $\epsilon=0.5$, $N=16$. (*a*) $\alpha=\pi/2$, $\beta=11\pi/254$; (*b*) $\alpha=-\pi/13$, $\beta=-\alpha$.

surface profiles are shown in figure 8 for $k_{B3}h=0.5$, $\epsilon=0.5$ ($\epsilon/\epsilon_*=0.5184$). Examples for $m=4$ are shown in figure 9 for $k_{B4}h=0.5$ and $\epsilon=0.5$ ($\epsilon/\epsilon_*=0.5104$). A few observations are made as follows.

First, in each case m, appropriate values of α and β can be found such that the amplitude of surface oscillation increases exponentially and monotonically along the channel. In figure 7(*a*), the surface amplitude at the right endwall is approximately 2.77 times than that at the left. For $m=3$ and $m=4$, the effects of Bragg resonance

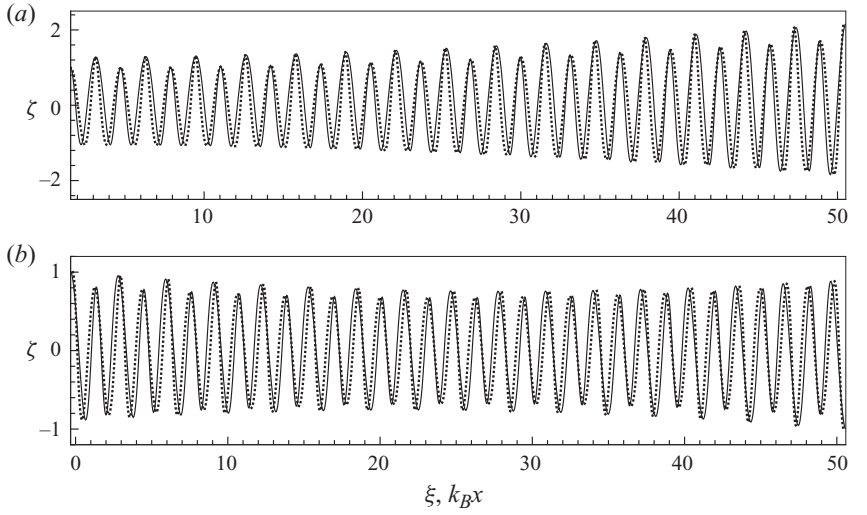

FIGURE 9. The profiles of the surface elevation (at $t = 0$) for quaternary Bragg resonance ($m = 4$): ——, as a function of ξ; ·····, as a function of $k_B x$. Parameters are $k_{B4}h = 0.5$, $\epsilon = 0.5$, $N = 16$. (*a*) $\alpha = \pi/2$, $\beta = 11\pi/254$; (*b*) $\alpha = -\pi/18$, $\beta = -\alpha$.

are limited when ϵ is small due to the narrow width of the resonance tongues. Nevertheless, with $\epsilon = 0.5$, the ratio of surface amplitudes at the two ends can be as large as 4.59 for $m = 3$, $k_{B3}h = 0.5$ in figure 8(*a*), and 2.16 for $m = 4$, $k_{B4}h = 0.5$ in figure 9(*a*). The three cases just mentioned are also listed in table 1, rows 1–3. The surface elevation ζ is the eigenvector for eigenvalue ω. For the normal modes in figures 7(*a*), 8(*a*) and 9(*a*), $\omega/\omega_{B2} = 0.9987$, $\omega/\omega_{B3} = 1.0199$ and $\omega/\omega_{B4} = 1.0124$, respectively. Note that ω_{Bm} is the frequency of the appropriate normal mode for the flat-bottom case. This is similar to the case $m = 1$ that Bragg resonance mostly affects the eigenfunction ζ but not the eigenvalue ω.

Second, when $\beta = -\alpha$ the eigenfunction ζ is symmetric with respect to the centre of the tank because of the symmetry of the geometry. With appropriate choice of α for each m, we see in figures 7(*b*), 8(*b*) and 9(*b*) that the surface amplitudes at the two endwalls are equal and decrease exponentially towards the minimum at the middle of the tank. For primary Bragg resonance ($m = 1$), it has been shown that for exponential modulation the spatial distribution of wave energy density depends sensitively on the precise positions of the endwalls relative to the corrugation crests (cf. HY07), confirming the results obtained using the asymptotic theory (Yu & Mei 2000*a*). This sensitive dependence is still true for higher order Bragg resonances, as seen from the results in figures 7–9, and in fact becomes more sensitive as m increases.

Third, for $m = 3$ and $m = 4$, the surface profiles show long-range exponential modulation due to Bragg resonances, as well as periodic modulations with a period of one (when m is even) or two (when m is odd) corrugation wavelengths. In figure 8(*a*) for $m = 3$, in addition to the general exponential decrease from right to left, one notices that every third peak is higher than its two neighbours, and every third trough is lower than its neighbours. (Half a cycle later, the lower troughs will be replaced by higher crests, of course.) Similarly, in figure 9(*a*) for $m = 4$, every other peak is higher than its neighbours. Since there are 16 corrugations in the tank, in figure 8(*a*) the two successive higher peaks are spaced by about two corrugation wavelengths, and in figure 9(*a*) they are spaced by about one corrugation wavelength.

N	m	$k_{Bm}h$	ϵ	ϵ/ϵ_*	β	a_R/a_L	ω/ω_{Bm}
16	2	0.5	0.3	0.3246	$17\pi/127$	2.7706	0.9987
16	3	0.5	0.5	0.5184	$11\pi/254$	4.5915	1.0199
16	4	0.5	0.5	0.5104	$11\pi/254$	2.1602	1.0124
10	2	0.5	0.3	0.3246	$14\pi/127$	1.8749	0.9983
10	3	0.5	0.5	0.5184	$6\pi/127$	2.6229	1.0214
10	4	0.5	0.5	0.5104	$4\pi/127$	1.6354	1.0125
8	2	0.5	0.3	0.3246	$12\pi/127$	1.6339	0.9986
8	2	0.5	0.5	0.5410	$14\pi/127$	4.3319	1.0043
4	2	0.5	0.5	0.5410	$12\pi/127$	2.0944	0.9977
8	3	0.5	0.6	0.6221	$6\pi/127$	3.7221	1.0280
6	3	0.5	0.6	0.6221	$6\pi/127$	2.7165	1.0309
4	3	0.5	0.6	0.6221	$6\pi/127$	2.0233	1.0384
8	4	0.5	0.6	0.6124	$6\pi/127$	2.3876	1.0149
6	4	0.5	0.6	0.6124	$4\pi/127$	1.9045	1.0182
4	4	0.5	0.6	0.6124	$2\pi/127$	1.4404	1.0218
8	2	0.9	0.4	0.5026	$16\pi/127$	2.2536	0.9945
8	2	0.9	0.6	0.7539	$13\pi/127$	6.6781	1.0056
8	3	0.9	0.5	0.5586	$6\pi/127$	2.0299	1.0159
8	3	0.9	0.6	0.6703	$5\pi/127$	3.4599	1.0213
8	4	0.9	0.5	0.5330	$4\pi/127$	1.4058	1.0052
8	4	0.9	0.6	0.6400	$6\pi/127$	2.2021	1.0064
8	2	1.2	0.3	0.4318	$12\pi/127$	1.3907	0.9967
8	2	1.2	0.5	0.7197	$16\pi/127$	3.0509	0.9948
8	3	1.2	0.4	0.4819	$11\pi/127$	1.2471	1.0048
8	3	1.2	0.6	0.7229	$7\pi/127$	2.9489	1.0088
8	4	1.2	0.5	0.5586	$5\pi/127$	1.3537	0.9997
8	4	1.2	0.6	0.6703	$7\pi/127$	2.0816	0.9986

TABLE 1. The ratio of the eigenfunction at the two endwalls, a_R/a_L, and the ratio of the frequency to ω_{Bm} for normal modes with exponential modulation. $\alpha = \pi/2$ in all examples, i.e. the left endwall is at a corrugation trough.

This short-range periodic modulation is due to the fact that the bottom corrugation is a spatial subharmonic of the water waves. The direct interaction of waves with the bottom, through the quadratic term in the boundary condition (2.2), produces spatial harmonics lower than the basic water waves, appearing as a subharmonic modulation of the basic waves. On the boundaries of the resonance tongues, when $\mu = 0$, long-range exponential modulation disappears and this subharmonic modulation is the only one present. On the other hand, for $m = 1$ and $m = 2$, the basic wave is the lowest harmonic in the Fourier series, and the direct interaction with the bottom produces the higher ones, which are usually regarded as distortions in the basic wave form.

Last, in computing the eigenfunctions, five pairs of evanescent modes have been used. It is found that these modes do not affect the surface profile significantly, even in the regions close to the endwalls. In figure 10, we show the normal velocity at the right endwall for the computed eigenfunction in figure 7(a). For comparison, we also compute the velocity by deliberately omitting the evanescent modes, using only the propagating modes. This is included in figure 10. The importance of the evanescent modes (i.e. fast varying flows) in satisfying the boundary condition is quite obvious. This is true in all cases for $m > 1$, consistent with the finding for $m = 1$ in HY07.

Other examples of computed normal modes with exponential modulation are listed in table 1, for different water depths, corrugation amplitudes and tank lengths. The ratios of surface amplitudes at the two endwalls are in column 7, showing the

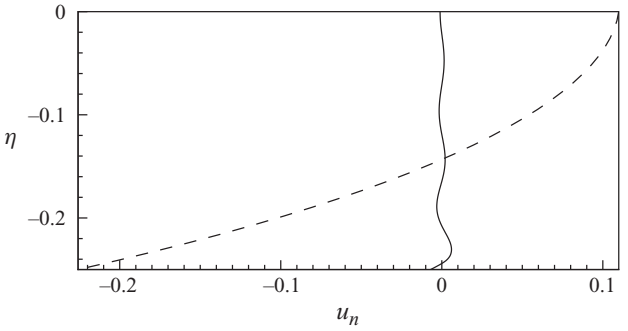

FIGURE 10. The normal velocity at the right endwall for the computed eigenfunction in figure 7(*a*): ——, using five pairs of evanescent modes and two propagating modes; – – –, using only the two propagating modes.

significance of the Bragg resonance effects. While both shallow water depth and a large number of corrugations are favourable for Bragg resonance, strong effects can still be seen in relatively deep waters or with as few as four corrugations.

5. Concluding remarks

Higher order Bragg resonances of water waves have been investigated, extending the exact solutions of linearized water waves over bottom corrugations of finite amplitude in HY07. These higher order Bragg resonances occur when the bottom corrugations have a spacing close to an integer multiple ($m > 1$) of half a water wavelength. For the Floquet-type solution, we have found the resonance tongues (ranges of water-wave frequencies) within which exponentially modulated propagating waves occur. Just outside a resonance tongue, but still sufficiently close to the mth Bragg resonance, sinusoidal modulations occur. These resonance tongues are cusps for $m > 1$ and wedges for $m = 1$ in the parameter plane of water-wave frequency versus corrugation amplitude ϵ, and tilted towards higher frequencies. The width of the cusp is of $O(\epsilon^m)$ for small ϵ. All these properties are similar to those of the Mathieu equation.

To illustrate the effects of these higher order Bragg resonances, we considered the normal modes of a rectangular tank. We have explored many examples, varying water depth, the amplitude and the number of bottom corrugations. While the effects become weaker at the higher order, even at $m = 4$ Bragg resonance can cause enough modulation of the standing wave that the surface amplitude at one end of the tank exceeds twice that at the other. This surface amplitude ratio depends sensitively on the endwall positions relative to the corrugation crests. This dependence, also seen in the $m = 1$ case in HY07, is consistent with the earlier studies of Bragg scattering by a finite number of sandbars in front of a (partially) reflective shoreline (Yu & Mei 2000*a*, *b*).

The particular bottom profile used in this study does have a Fourier series containing harmonics $\cos(2nk_B x)$, $n = 1, 2, \ldots$. However, it should be emphasized that the $m > 1$ resonances just examined cannot be interpreted as if they were $m = 1$ resonance by the higher harmonic components of the bottom, as the processes have different behaviour (see the Appendix). It may be possible for one to imagine that an mth-order resonance by a periodic bottom is a mixture of different order scattering processes by individual bottom harmonic components, but it is not clear at all if one can possibly separate, and hence quantify the contributions of, these individual scattering processes in a

physically meaningful way. This is because there is no linearity with respect to the bottom shape, even when the fluid motion is linear: one cannot add a solution for $h_{b1} = 0.2h\cos(2k_B x)$ to one for $h_{b2} = 0.1h\cos(4k_B x)$ to get a solution for the profile $h_{b1} + h_{b2}$. The fact that a periodic bottom can be represented by a Fourier series does not mean that wave scattering can be described as any kind of superposition of that by some basic set of special bottom shapes like $\cos(2nk_B x)$. It then seems better to just treat a periodic bottom with an identified fundamental wavenumber (shortest spatial period), say $2k_B$, and examine the properties of water waves of frequencies close to $\omega_{Bm}^2 = gk_{Bm}\tanh k_{Bm}h$, $m = 1, 2, \ldots$. The bottom profile given parametrically by (2.4) appears to be one of the simplest periodic forms for which exact solutions (neither perturbative nor purely numerical) can be developed, as shown in HY07 and here.

The Floquet solutions of HY07, further developed here, can be used to study different problems of linear water waves passing over a patch of corrugations, with boundary or matching conditions at its ends appropriate to the physical setting of interest. Whenever the wave frequency is near one of the Bragg resonances, the rate of exponential modulation (Floquet exponent) may be large enough to cause significant variations of wave amplitude over the possibly fairly short patch, as in our illustrative normal-mode examples. In nature, multiple parallel sandbars do occur. They may be primary Bragg resonant with some ocean waves and $m > 1$ resonant with some others. The present study of non-erodible bottom corrugations can be useful in understanding sediment processes and seabed evolution. Yu & Mei (2000*b*) showed that Bragg scattering by evolving sandbars can be treated as if the bars were rigid because the time scale for sediment morphodynamics is much longer than that of the waves. They found that during the course of sandbar formation all the possible spatial variations of wave amplitude uncovered in their earlier study of rigid bars (Yu & Mei 2000*a*) occurred at different stages of the evolution, as the position of the bar crests relative to the waves evolves.

Some limitations of the exact theory have been remarked on in HY07, e.g. lack of effects of dissipation and nonlinearity of the free surface. Nonetheless, the theoretical results presented here provide some insights into wave interaction with periodic undulating seabed topography. They can also be of use to those who are interested in experimental studies of Bragg resonances of water waves.

Support of J. Y. by the US National Science Foundation (Grant CBET-0756271) and the North Carolina Sea Grant (Grant R/MG-0707) during the period of this work is gratefully acknowledged.

Appendix

The bottom corrugation defined in (2.4) is not purely sinusoidal, containing harmonics $\cos(2nk_B x)$, $n = 1, 2, \ldots$. Here we show that the higher order resonance addressed in this study is not due to the first-order Bragg resonance by these higher harmonic components in the bottom profile. Some quantitative differences can be seen by examining the width of the resonance tongue and the Floquet exponent. We shall use the case $m = 2$ as an example.

For small ϵ, the bottom profile (2.4) can be approximated as

$$h_b = \epsilon h\cos(2k_B x) + \epsilon^2 k_B h^2 \coth(2k_B h)\,[\cos(4k_B x) - 1] + \cdots. \tag{A 1}$$

The amplitude of the first bottom harmonic is ϵh, and that of the second harmonic is $\epsilon^2 k_B h^2 \coth(2k_B h)$. We do not know the exact solution for purely sinusoidal bottom shapes, but to the lowest order in amplitude we can use the asymptotic theory, which has been shown to agree well with the exact theory on the slowly varying aspects of the flows (i.e. propagating modes).

For $m=1$ Bragg resonance of the water wave by a purely sinusoidal bottom, the boundaries of the resonance tongue are $\omega_{c\mp}/\omega_B = 1 \mp (1/2)(\epsilon b)$, and hence the width $(\omega_{c+} - \omega_{c-})/\omega_B = \epsilon b$ (cf. HY07, §4.1). The parameter b is the same as in (2.8). Thus, to estimate the resonance tongue of $m=1$ resonance by a bottom shape given by the second bottom harmonic in (A 1), we identify ω_B with ω_{B2}, ϵ with $\epsilon' = \epsilon^2 k_B h \coth(2k_B h)$ and b with $b' = k_{B2}h/\sinh k_{B2}h$, thus obtaining

$$\omega'_{c\mp}/\omega_{B2} = 1 \mp \tfrac{1}{2}(\epsilon' b') = 1 \mp \tfrac{1}{2}(\epsilon b)^2, \tag{A 2}$$

and hence the width is $(\omega'_{c+} - \omega'_{c-})/\omega_{B2} = (\epsilon b)^2$. According to the exact theory, the width of the resonance tongue of $m=2$ resonance is also $(\omega_{c+} - \omega_{c-})/\omega_{B2} = (\epsilon b)^2$ when ϵ is small (cf. (3.8)). However, the boundaries are (cf. (3.8))

$$\omega_{c\mp}/\omega_{B2} = 1 + \tfrac{1}{2}(\epsilon b)^2\left[(1 \mp 1) + (1 - \lambda_{B4}/\lambda_{B2})^{-1}\right]. \tag{A 3}$$

For large $k_B h$, $\lambda_{B4}/\lambda_{B2} \simeq 2$, and (A 3) and (A 2) are approximately the same. For small $k_B h$, however, $\lambda_{B4}/\lambda_{B2} \simeq 4$; so $\omega_{c-}/\omega_{B2} = 1 - (1/6)(\epsilon b)^2$ and $\omega_{c+}/\omega_{B2} = 1 + (5/6)(\epsilon b)^2$.

For $m=1$ resonance by a bottom shape given by the second bottom harmonic in (A 1), the Floquet exponent is estimated as (cf. (4.1) in HY07)

$$\mu'^2 = \left(b' + \tfrac{1}{2}\right)^{-2}\left(\tfrac{1}{4}(\epsilon' b')^2 - \left[(\lambda/\lambda_{B2})^{1/2} - 1\right]^2\right).$$

For $\lambda/\lambda_{B2} = 1$,

$$\mu'^2 = \frac{1}{4}(\epsilon b)^4\left(\frac{1}{2} + \frac{2k_B h}{\sinh 4k_B h}\right)^{-2}. \tag{A 4}$$

According to the exact theory, the Floquet exponent for $m=2$ Bragg resonance is, from (3.5) and (3.6), for small ϵ and $\lambda/\lambda_{B2} = 1$

$$\mu^2 = (\epsilon b)^4\left(\frac{1}{2} + \frac{2k_B h}{\sinh 4k_B h}\right)^{-2}\left[1 - \left(1 + \frac{\lambda_{B2}}{\lambda_{B2} - \lambda_{B4}}\right)^2\right]. \tag{A 5}$$

For $k_B h \ll 1$, the factor $1 - (1 + \lambda_{B2}/(\lambda_{B2} - \lambda_{B4}))^2 \to 5/9$, and for $k_B h \gg 1$, it approaches 1. The Floquet exponent μ^2 for $m=1$ Bragg resonance by the second harmonic alone is nearly two times smaller than that for $m=2$ resonance by the actual bottom when $k_B h$ is small, and four times smaller when $k_B h$ is large.

REFERENCES

Abramowitz, M. & Stegun, I. A. 1964 *Handbook of Mathematical Functions*. National Bureau of Standards, Applied Mathematics Series 55. US Government Printing Office.

Alam, M.-R., Liu, Y. & Yue, D. K. P. 2009 Bragg resonance of waves in a two-layer fluid propagating over bottom ripples. Part 1. Perturbation analysis. *J. Fluid Mech.* **624**, 191–224.

Bragg, W. H. & Bragg, W. L. 1913 The reflection of X-rays by crystals. *Proc. R. Soc. Lond.* A **88** (605), 428–438.

Dalrymple, R. A. & Kirby, J. T. 1986 Water waves over ripples. *J. Waterw. Port Coast. Ocean Engng Div. ASCE* **112**, 309–319.

Davies, A. G. 1982 The reflection of the wave energy by undulations of the seabed. *Dyn. Atmos. Oceans* **6**, 207–232.

Davies, A. G., Guazzelli, E. & Belzons, M. 1989 The propagation of long waves over an undulating bed. *Phys. Fluids* A **1**, 1331–1340.

Davies, A. G. & Heathershaw, A. D. 1984 Surface wave propagation over sinusoidally varying topography. *J. Fluid Mech.* **144**, 419–443.

Guazzelli, E., Rey, V. & Belzons, M. 1992 Higher-order Bragg reflection of gravity surface waves by periodic beds. *J. Fluid Mech.* **245**, 301–317.

Howard, L. N. & Yu, J. 2007 Normal modes of a rectangular tank with corrugated bottom. *J. Fluid Mech.* **593**, 209–234.

Kirby, J. T. 1986 A general wave equation for waves over rippled beds. *J. Fluid Mech.* **162**, 171–186.

Kirby, J. T. 1989 Propagation of surface waves over an undulating bed. *Phys. Fluids* A **1**, 1898–1899.

Liu, P. L.-F. 1987 Resonant reflection of water waves in a long channel with corrugated boundaries. *J. Fluid Mech.* **179**, 371–381.

Liu, Y. & Yue, D. K. P. 1998 On generalized Bragg scattering of surface waves by bottom ripples. *J. Fluid Mech.* **356**, 297–326.

Mathieu, É. 1868 Mémoire sur le mouvement vibratoire d'une membrane de forme elliptique. *J. Math. Pure Appl.* **13**, 137–203.

Mei, C. C. 1985 Resonant reflection of surface waves by periodic sandbars. *J. Fluid Mech.* **152**, 315–337.

Mei, C. C., Hara, T. & Naciri, M. 1988 Note on Bragg scattering of water waves by parallel bars on the seabed. *J. Fluid Mech.* **186**, 147–162.

Phillips, O. M. 1960 On the dynamics of unsteady gravity waves of finite amplitude. Part 1. *J. Fluid Mech.* **9**, 193–217.

Phillips, O. M. 1977 *The Dynamics of the Upper Ocean*. Cambridge University Press.

Rey, V., Guazzelli, E. & Mei, C. C. 1996 Resonant reflection of surface gravity waves by one-dimensional doubly sinusoidal beds. *Phys. Fluids* **8**, 1525–1530.

Yu, J. & Mei, C. C. 2000*a* Do longshore bars shelter the shore? *J. Fluid Mech.* **404**, 251–270.

Yu, J. & Mei, C. C. 2000*b* Formation of sand bars under surface waves. *J. Fluid Mech.* **416**, 315–348.